

# Model Experiment on Heel-Induced Hydrodynamic Forces in Waves for Broaching Prediction

Hirotsada HASHIMOTO<sup>\*1</sup>, Naoya UMEDA<sup>\*1</sup> and Akihiko MATSUDA<sup>\*2</sup>

<sup>\*1</sup> Osaka University, Yamadaoka, Suita, 565-0871, Japan

*h\_hashi@naoe.eng.osaka-u.ac.jp, umeda@naoe.eng.osaka-u.ac.jp*

<sup>\*2</sup> National Research Institute of Fisheries Engineering, Hasaki, Kashima, 314-0421, Japan

*amatsuda@fra.affrc.go.jp*

## ABSTRACT

Nowadays, theoretical prediction of extreme motions in following and quartering seas is required not only for qualitative purposes but also for quantitative one towards direct stability assessment as an alternative route of IMO IS Code. The mathematical model for capsizing due to broaching, one of the great threat to ships running in following and quartering seas, has been developed by many researchers. However these models can predict it only qualitatively. For realising more quantitative prediction, the effect of nonlinear heel-induced hydrodynamic forces in calm water was examined by the authors in their previous work. In this research, we conduct the systematic captive model experiments with the various heel angles up to the 50 degrees in severe following waves. As a result, the details of nonlinear heel-induced hydrodynamic forces with respect to heel angle in waves are presented. Then the comparisons between the free running model experiments and numerical simulations with direct use of the heel-induced hydrodynamic sway force and yaw moment are carried out. These comparisons are conducted in time series and boundaries of ship motion modes. Finally the comparisons between the mathematical model with experimentally obtained GZ variation in waves and that with theoretically obtained one are conducted for discussing the possibility of realising more quantitative prediction of extreme ship motions in following and quartering seas.

## KEYWORDS

New captive model experiment, Heel-induced hydrodynamic forces in waves, Numerical prediction of broaching

## INTRODUCTION

Recent model experiments (e.g. Umeda et al. 1999) demonstrate that a ship complying with the current Intact Stability Code (IS Code) of International Maritime Organisation (IMO) rarely capsizes in non-breaking beam waves but could occasionally capsize when she runs in following and quartering seas. Although the IMO circulated a simple guidance applicable to all ships for avoiding danger in following and quartering seas, real capsizing boundaries might depend on detailed particulars of each ship. Responding to these situations the Sub-Committee on stability, load lines and on fishing vessel safety has started to review the IS Code. On this revision, an alternative approval of safety with direct assessment by physical or numerical tests is considered. This kind of assessment of safety is especially expected to prevent ship capsizing due to broaching in following and quartering seas. This is because the existing stability criteria cannot deal with this phenomenon, which depends on hull form details as well as operational practices. At this stage numerical models are required to provide not only qualitative agreement but also quantitative one with help of model experiments. Toward this direction, the International Towing Tank Conference (ITTC) had conducted benchmark testing of several numerical models by comparing them with existing capsizing model experiments in following and quartering seas, which cover ship capsizes due to parametric rolling and broaching. As a result, it was confirmed that only a few numerical models could qualitatively predict capsizing and none could do it quantitatively (Umeda et al. 2001). Therefore, existing numerical modelling techniques should

be upgraded to realise a quantitative prediction of capsizing. For this purpose, it is necessary to systematically examine all factors relevant to capsizing in following and quartering seas further.

It has been pointed out that the effect of heel-induced manoeuvring forces is significant for broaching prediction. (Renilson et al. 2000) This effect was taken into account as linear function of roll angle and their derivatives were obtained from captive model test with small heel angle in still water. However the relationship between heel-induced hydrodynamic forces and roll angles could be nonlinear because under-water hull form becomes quite asymmetric with increasing of roll angle. Therefore it is important to conduct systematic model experiment to measure heel-induced hydrodynamic forces especially with large heel angle. However this kind of experiment is quite difficult because of the limitation of experimental setup. Within a framework of ordinal procedure and setup, problems of water-inflow and water-accumulation in a hull cannot avoid. To overcome these problems, using complete watertight ship model or devices to prevent a dynamometer to be flooded is required. In past Nakato et al. conducted a captive model experiment with special setup that a dynamometer is settled quite higher position than the centre of gravity of a ship model to measure restoring moments in waves with a wide range of roll angle. (Nakato et al. 1990) However their experimental method and results were not available to practical use because a dynamometer settled at high position provides significant trim moment in running. For these reasons, a captive model experiment to measure hydrodynamic forces induced by large heel is quite difficult even in still water. Therefore it is important to develop an experimental procedure to directly measure these forces in both still water and waves.

In our previous work, we had proposed a new experimental method with a purpose-built ship model and an experimental setup, which can realise captive tests up to 90 degrees of heel. (Hashimoto et al. 2004) Then captive tests were conducted to measure heel-induced hydrodynamic forces in still water. In this paper captive model tests to measure heel-induced hydrodynamic forces in heavy following waves were conducted. Based on these results, the mathematical model is enhanced by introducing nonlinear model of hydrodynamic forces as functions of roll angle, and is applied to prediction of ship motions in following and quartering waves. The comparison of the 4 DOF mathematical models with and without this effect is conducted, together with the existing free-running experiments, to examine the importance of nonlinear heel-induced hydrodynamic forces in waves on prediction of ship capsizing due to broaching in following and quartering seas.

## **A NEW CAPTIVE MODEL EXPERIMENT WITH LARGE HEEL**

### ***Procedure of an Experiment***

For measuring heel-induced hydrodynamic forces with large heel, a new 1/25 scaled model of the 135GT Japanese purse seiner was built. Its body plan, general arrangement of a ship model and principal particulars are shown in Fig.1, Fig.2 and Table.1, respectively. Here smaller model size was selected to consider a maximum loading allowance of the dynamometer in case whole of a ship model is in air. The ship model is completely watertight and has bulwarks, freeing ports and the super structures that are similar to the ship model used in free-running model experiment (Umeda et al. 1999). There are two poles, having a scale, that fix the model and adjust a model attitude. Each pole has gimbals at their bottom to realize a specified heel angle. Captive model experiments were conducted at a seakeeping and manoeuvring basin of National Research Institute of Fisheries Engineering. The model was towed by a main towing carriage in long-crested regular waves, and model was equipped with a rudder but without a propeller. The model was completely fixed by two poles in all directions. Because a ship model is fixed, only one data for certain relative position of a wave is obtained per one running of towing carriage. In this experiment heel-induced hydrodynamic forces in waves are identified by measuring eight relative positions of a wave with same heel angle. Surge force, sway force, heave force, roll moment, pitch moment and yaw moment acting on the towed model were detected by a dynamometer located in vertically high position where no water-splash occurs.

Procedure of the experiment is as follows. Firstly instantaneous heave and pitch with no heel are estimated for certain relative position of a wave from tests with conventional setup in moderate wave steepness. Since wave steepness is different from desired value, we estimate a ship instantaneous heave and pitch by assuming linearity of them with respect to wave steepness. The effect of heel is added with Froude-Krylov assumption. Here the calculation is obtained by integrating undisturbed wave pressure up to the wave surface with the Smith effect for a ship free in heave and pitch. By adjusting a length of two poles and an angle of gimbals, a sinkage, trim and heel angle are set to be equal to the estimated values. An example photograph of this experimental setup is shown in Fig.3. Here estimated ship attitude does not usually correspond to the real one. However it is quite difficult to accurately estimate a ship attitude with large heel and high forward velocity in steep waves. To correct this difference, additional experiments are carried out for obtaining derivatives of heel-induced hydrodynamic forces with respect to sinkage and trim angle. If we conduct this additional experiment to all relative positions and heel angles, the number of model runs could be prohibitively large. To avoid this problem, we apply the following method. As mentioned we repeat eight model runs to measure heel-induced hydrodynamic forces for one wave. Because a ship model is slowly overtaken by waves, the other seven data measured with undesired ship attitude is available to obtain derivatives of hydrodynamic forces with respect to sinkage and trim at specified relative position. Using such derivatives we can reasonably estimate all forces and moments in the case that ship is free in heave and pitch by solving the simultaneous equations satisfying that heave force and pitch moment equal to zero.

Table.1 Principal particulars of the subject ship

<i>Items</i>	<i>Values</i>
length : $L_{pp}$	34.5 m
breadth : $B$	7.60 m
depth : $D$	3.07 m
mean draught : $d$	2.65 m
block coefficient : $C_b$	0.597
longitudinal position of centre of gravity from the midship : $x_{CG}$	1.31 m aft
metacentric height : $GM$	1.00 m
natural roll period : $T$	7.4 s
rudder area : $A_R$	3.49 m <sup>2</sup>
time constant of steering gear : $T_E$	0.63 s
proportional gain: $K_p$	1.0
time constant for differential control: $T_D$	0.0 s
maximum rudder angle: $\delta_{max}$	$\pm 35^\circ$

### Procedure of an Analysis

The surge force,  $X$ , the sway force,  $Y$ , the heave force,  $Z$ , the roll moment,  $K$ , the pitch moment,  $M$  and the yaw moment,  $N$ , were measured as functions of heave, pitch, roll, Froude number and the horizontal position of ship to a wave trough,  $\xi_G/\lambda$ . Wave height at a centre of ship gravity was also measured by a servo-needle wave probe. The definition of directions of the measured forces and moments is shown in Fig.4. All forces and moments were measured in horizontal axes. Each moment is geometrically converted from the measured value around the centre of the dynamometer to that of ship gravity. By assuming that additional change in sinkage and trim are small the measured forces and moments can be expanded as follows:

$$X(\zeta_G, \theta, \phi, F_n, \xi_G / \lambda) = X(\zeta_{G0}, \theta_0, \phi, F_n, \xi_G / \lambda) + X_\zeta(\zeta_{G0}, \theta_0, \phi, F_n, \xi_G / \lambda) \times \zeta_G^* + X_\theta(\zeta_{G0}, \theta_0, \phi, F_n, \xi_G / \lambda) \times \theta^* \quad (1)$$

$$Y(\zeta_G, \theta, \phi, F_n, \xi_G / \lambda) = Y(\zeta_{G0}, \theta_0, \phi, F_n, \xi_G / \lambda) + Y_\zeta(\zeta_{G0}, \theta_0, \phi, F_n, \xi_G / \lambda) \times \zeta_G^* + Y_\theta(\zeta_{G0}, \theta_0, \phi, F_n, \xi_G / \lambda) \times \theta^* \quad (2)$$

$$Z(\zeta_G, \theta, \phi, F_n, \xi_G / \lambda) = Z(\zeta_{G0}, \theta_0, \phi, F_n, \xi_G / \lambda) + Z_\zeta(\zeta_{G0}, \theta_0, \phi, F_n, \xi_G / \lambda) \times \zeta_G^* + Z_\theta(\zeta_{G0}, \theta_0, \phi, F_n, \xi_G / \lambda) \times \theta^* \quad (3)$$

$$K(\zeta_G, \theta, \phi, F_n, \xi_G / \lambda) = K(\zeta_{G0}, \theta_0, \phi, F_n, \xi_G / \lambda) + K_\zeta(\zeta_{G0}, \theta_0, \phi, F_n, \xi_G / \lambda) \times \zeta_G^* + K_\theta(\zeta_{G0}, \theta_0, \phi, F_n, \xi_G / \lambda) \times \theta^* \quad (4)$$

$$M(\zeta_G, \theta; \phi, F_n, \xi_G / \lambda) = M(\zeta_{G0}, \theta_0; \phi, F_n, \xi_G / \lambda) + M_\zeta(\zeta_{G0}, \theta_0; \phi, F_n, \xi_G / \lambda) \times \zeta_G^* + M_\theta(\zeta_{G0}, \theta_0; \phi, F_n, \xi_G / \lambda) \times \theta^* \quad (5)$$

$$N(\zeta_G, \theta; \phi, F_n, \xi_G / \lambda) = N(\zeta_{G0}, \theta_0; \phi, F_n, \xi_G / \lambda) + N_\zeta(\zeta_{G0}, \theta_0; \phi, F_n, \xi_G / \lambda) \times \zeta_G^* + N_\theta(\zeta_{G0}, \theta_0; \phi, F_n, \xi_G / \lambda) \times \theta^* \quad (6)$$

Here

$$\zeta_G^* = \zeta_G - \zeta_{G0} \quad (7)$$

$$\theta^* = \theta - \theta_0 \quad (8)$$

where  $\zeta_{G0}$  and  $\theta_0$  indicate the sinkage and trim angle, respectively, initially estimated. If ship model is free in heave and pitch, heave force and pitch moment should be zero. Therefore  $\zeta_G^*$ ,  $\theta^*$  can be obtained by solving following simultaneous equations.

$$Z(\zeta_{G0}, \theta_0; \phi, F_n, \xi_G / \lambda) + Z_\zeta(\zeta_{G0}, \theta_0; \phi, F_n, \xi_G / \lambda) \zeta_G^* + Z_\theta(\zeta_{G0}, \theta_0; \phi, F_n, \xi_G / \lambda) \theta^* = 0 \quad (9)$$

$$M(\zeta_{G0}, \theta_0; \phi, F_n, \xi_G / \lambda) + M_\zeta(\zeta_{G0}, \theta_0; \phi, F_n, \xi_G / \lambda) \zeta_G^* + M_\theta(\zeta_{G0}, \theta_0; \phi, F_n, \xi_G / \lambda) \theta^* = 0 \quad (10)$$

Then, the surge force and sway force, roll moment and yaw moment for the case in which model is free in heave and pitch can be estimated with Equations (1), (2), (4) and (6).

## EXPERIMENTAL RESULTS

Captive model experiments to measure heel-induced hydrodynamic forces in following waves were conducted. Wave condition is selected to correspond to that of ITTC Benchmark Testing Programme,  $H/\lambda=1/10$  and  $\lambda/L=1.637$ . Captive tests were conducted for various sets of heel angle with Froude number of 0.4. Here heel angles are 0, 10, 20, 30, 40 and 50 degrees. Heel-induced hydrodynamic surge force, sway force, yaw moment and roll moment in waves are obtained by subtracting a constant value obtained in still water with each heel angle. Finally these results are identified by the Fourier expansion with encounter frequency. An example photograph of this experiment is shown in Fig.5.

The experimental results of non-dimensional heel-induced surge force,  $\Delta X'$ , sway force,  $\Delta Y'$ , yaw moment,  $\Delta N'$ , and roll moment,  $\Delta K'$ , in following waves with  $Fn=0.4$  are shown in Figs.6-9. The amplitude of  $\Delta X'$  linearly increases with respect to roll angle and the phase of  $\Delta X'$  drastically changes. Although the reason is not clarified in this moment, the amplitude of  $\Delta X'$  itself is much smaller than the variation of wave-induced surge force with no heel angle. Therefore heel-induced surge force in waves can be neglected for numerical prediction. The amplitude of  $\Delta Y'$  linearly increases up to 20 degrees of heel but does nonlinearly over 20 degrees of heel. The phase of  $\Delta Y'$  also changes with respect to roll angle.  $\Delta N'$  and  $\Delta K'$  have similar tendency in its change as  $\Delta Y'$ , nonlinearity with increasing of roll angle appears over 20 degrees of heel. Since  $\Delta K'$  seems to be important for capsizing prediction, a comparison of roll restoring moment in waves between the experimental result, the Froude-Krylov calculation and the sum of Froude-Krylov calculation and experimental formula of lift effect (Umeda et al. 2002). Here the Froude-Krylov calculation is conducted by integrating undisturbed wave pressure up to the wave surface with the Smith effect for a ship free in heave and pitch. Fig.10 shows a comparison of GZ curve between experiment and two calculations. Froude-Krylov calculation overestimates the amplitude of GZ variation. There is significant difference in the average value and phase of GZ variation. The experimentally obtained relative position of minimum GZ is not wave crest but wave down-slope. Calculation by Froude-Krylov assumption corrected by the experimental formula can predict these tendencies. However the difference from experimental result is not negligibly small from a viewpoint of realising a quantitative prediction. Therefore a proposed captive model experiment is recommended to accurately predict a wave effect on roll restoring moment in severe waves.

## MATHEMATICAL MODELLING

The mathematical model of the surge-sway-yaw-roll motion was developed by Umeda and Renilson (Umeda et al. 1992) and Umeda (Umeda 1999) for capsizing associated with surf-riding in following and quartering waves. The details of this model can be found in the literature (Umeda et al. 2002). Although this model had consistently ignored higher order terms of waves, several higher order terms were added in the previous paper (Hashimoto et al.

2004). Then heel-induced hydrodynamic forces measured in waves are added in this research. Two co-ordinate systems used here are shown in Fig.11: (1) a wave fixed with its origin at a wave trough, the  $\xi$  axis in the direction of wave travel; and (2) an upright body fixed with its origin at the centre of ship gravity. The state vector,  $\mathbf{x}$  and control vector,  $\mathbf{b}$ , of this system are defined as follows.

$$\mathbf{x} = (x_1, x_2, \dots, x_8)^T = \{\xi_G / \lambda, u, v, \chi, r, \phi, p, \delta\}^T \quad (11)$$

$$\mathbf{b} = \{n, \chi_c\}^T \quad (12)$$

The dynamical system can be represented by the following state equation.

$$\dot{\mathbf{x}} = \mathbf{F}(\mathbf{x}; \mathbf{b}) = \{f_1(\mathbf{x}; \mathbf{b}), f_2(\mathbf{x}; \mathbf{b}), \dots, f_8(\mathbf{x}; \mathbf{b})\}^T \quad (13)$$

where

$$f_1(\mathbf{x}; \mathbf{b}) = (u \cos \chi - v \sin \chi - c) / \lambda \quad (14)$$

$$f_2(\mathbf{x}; \mathbf{b}) = \{T(u; n) + T^W(\xi_G / \lambda, u, \chi; n) - R(u) + X^R_{NL}(u, \phi) + X^M_{NL}(u, v, r; n) + X_{nd}(\xi_G / \lambda, u, \chi, \delta; n) + X_w(\xi_G / \lambda, \chi)\} / (m + m_x) \quad (15)$$

$$f_3(\mathbf{x}; \mathbf{b}) = \{-(m + m_x)ur + Y_v(u; n)v + Y_v^W(\xi_G / \lambda, u, \chi; n)v + Y_r(u; n)r + Y_r^W(\xi_G / \lambda, u, \chi; n)r + Y^M_{NL}(u, v, r; n) + Y_\phi(u)\phi + Y^{RW}_{NL}(u, \phi) + \underline{Y^{RW}_{NL}(\xi_G / \lambda, \chi, \phi)} + Y_\delta(u; n)\delta + Y_\delta^W(\xi_G / \lambda, u, \chi; n)\delta + Y_w(\xi_G / \lambda, u, \chi; n)\} / (m + m_y) \quad (16)$$

$$f_4(\mathbf{x}; \mathbf{b}) = r \quad (17)$$

$$f_5(\mathbf{x}; \mathbf{b}) = \{N_v(u; n)v + N_v^W(\xi_G / \lambda, u, \chi; n)v + N_r(u; n)r + N_r^W(\xi_G / \lambda, u, \chi; n)r + N^M_{NL}(u, v, r; n) + N_\phi(u)\phi + N^R_{NL}(u, \phi) + \underline{N^{RW}_{NL}(\xi_G / \lambda, \chi, \phi)} + N_\delta(u; n)\delta + N_\delta^W(\xi_G / \lambda, u, \chi; n)\delta + N_w(\xi_G / \lambda, u, \chi; n)\} / (I_{zz} + J_{zz}) \quad (18)$$

$$f_6(\mathbf{x}; \mathbf{b}) = p \quad (19)$$

$$f_7(\mathbf{x}; \mathbf{b}) = [m_x z_H(u, v)ur + K_v(u, v; n)v + K_v^W(\xi_G / \lambda, u, v, \chi; n)v + K_r(u, v; n)r + K_r^W(\xi_G / \lambda, u, v, \chi; n)r + K^M_{NL}(u, v, r; n) + K_p(u)p + K_\phi(u)\phi + K^R_{NL}(u, \phi) + K_\delta(u; n)\delta + K_\delta^W(\xi_G / \lambda, u, \chi; n)\delta + K_w(\xi_G / \lambda, u, \chi; n) - mg\{GZ(\phi) + \underline{GZ^{RW}(\xi_G / \lambda, \chi, \phi)}\}] / (I_{xx} + J_{xx}) \quad (20)$$

$$f_8(\mathbf{x}; \mathbf{b}) = \{-\delta - K_R(\chi - \chi_c) - K_R T_D r\} / T_E \quad (21)$$

Here the underlined parts indicate the heel-induced hydrodynamic forces newly added to the previous model. Here the Grim's effective wave concept (Grim 1961) is used for estimation of heel-induced hydrodynamic forces in waves with heading angle. In numerical simulation, heel-induced hydrodynamic forces obtained in still water are also taken into account. Although the experimental results shown in Figs.6-9 are obtained for only one Froude number, we assume that these results are applicable to all Froude number cases because of the limitation of available experimental data.

## NUMERICAL RESULTS

Firstly the comparisons between the numerical results with nonlinear heel-induced hydrodynamic sway force and yaw moment in waves and without them as well as existing free running model experiments (Umeda et al 1999) are conducted. The comparison in the case that the ship experiences a periodic motion is shown in Fig.12. The difference between calculated results with and without nonlinear heel-induced hydrodynamic sway force and yaw moment is not so significant. The comparison in the case that the ship suffers surf-riding, broaching and capsizing is shown in Fig.13. Although the mathematical model with nonlinear heel-induced hydrodynamic sway force and yaw moment provides slightly longer time to capsize, prediction accuracy of two models is almost the same. Comparison in boundaries of ship motion modes for control parameters of auto pilot course and nominal Froude number is shown in Fig.14. The procedure of this calculation can be found in the literature (Umeda et al. 2002). In the numerical results, a region of capsizing due to broaching becomes smaller and that of stable surf-riding does larger by taking the heel-induced hydrodynamic sway force and yaw moment into account. There is no significant difference between two models in the prediction accuracy of critical Froude number of ship capsizing. These results suggest that the effect of the heel-induced hydrodynamic sway force and yaw moment in waves can be neglected for practical broaching prediction.

Secondly the comparison between the mathematical model with experimentally obtained variation of roll restoring moment in waves and that with theoretically obtained one. Here theoretical prediction is based on the Froude-Krylov assumption with the correction by experimental formula of heel-induced lift effect. The comparison in the case that the ship experiences a periodic motion is shown in Fig.15. No significant difference is found but the amplitude of roll motion is different to some extent. The comparison in the case that the ship suffers surf-riding, broaching and capsizing is shown in Fig.16. The results seem to be almost the same despite of the difference of GZ variation. Comparison in boundaries of ship motion modes for control parameters is shown in Fig.17. There is significant difference in the prediction of critical ship speed of capsizing especially at larger auto pilot course and better agreement with free running model experiments can be found in the prediction with experimentally obtained variation of roll restoring in waves. Because the experimental formula is obtained only from the tests with 10 degrees of heel in following seas, it is not adequate to apply this formula to the case with large roll angle and large heading angle. These results suggest that accurate estimation of GZ variation in severe waves is indispensable for realising a quantitative capsizing prediction.

## CONCLUSIONS

Nonlinear heel-induced hydrodynamic forces in following waves are measured by a new experimental method with a purpose-built ship model and setup. Then a mathematical model taking these forces into account is developed, and is compared with existing free running experiments. As a result, the following conclusions are obtained:

1. The proposed experimental method is applicable to measure heel-induced hydrodynamic forces with large heel angle even in severe waves.
2. Heel-induced hydrodynamic surge force in waves is small and can be neglected for capsizing prediction.
3. Heel-induced hydrodynamic sway force, yaw moment and roll moment in waves have certain nonlinearity with respect to roll angle especially over 20 degrees of heel.
4. Heel-induced hydrodynamic sway force and yaw moment in waves are not so significant for capsizing prediction.
5. Accurate prediction of GZ variation of running ship in waves is important for capsizing prediction.

## ACKNOWLEDGMENTS

This research was supported by a Grant-in Aid for Scientific Research of the Ministry of Education, Culture, Sports, Science and Technology of Japan (No. 15360465) and a Fundamental Research Developing Association for Shipbuilding and Offshore of the Shipbuilders' Association of Japan.

## NOMENCLATURE

$c$	wave celerity
$F_n$	nominal Froude number
$GZ$	righting arm
$GZ^{RW}$	heel-induced variation of righting arm in waves
$H$	wave height
$I_{xx}$	moment of inertia in roll
$I_{zz}$	moment of inertia in yaw
$J_{xx}$	added moment of inertia in roll
$J_{zz}$	added moment of inertia in yaw
$K_{NL}^M$	nonlinear manoeuvring forces in roll
$K_{NL}^R$	nonlinear heel-induced hydrodynamic roll moment in still water
$K_p$	derivative of roll moment with respect to roll rate
$K_r$	derivative of roll moment with respect to yaw rate
$K_r^W$	wave effect on the derivative of roll moment with respect to yaw rate
$K_R$	rudder gain
$K_v$	derivative of roll moment with respect to sway velocity
$K_v^W$	wave effect on the derivative of roll moment with respect to sway velocity
$K_w$	wave-induced roll moment

$K_\delta$	derivative of roll moment with respect to rudder angle
$K_\delta^W$	wave effect on the derivative of roll moment with respect to rudder angle
$K_\phi$	derivative of roll moment with respect to roll angle
$\Delta K'$	$\Delta K' = \Delta K / (1/2 \rho L d^2 u^2)$
$L$	ship length between perpendiculars
$m$	ship mass
$m_x$	added mass in surge
$m_y$	added mass in sway
$n$	propeller revolution number
$N_{NL}^M$	nonlinear manoeuvring forces in yaw
$N_{NL}^R$	nonlinear heel-induced hydrodynamic yaw moment in still water
$N_{NL}^{RW}$	nonlinear heel-induced hydrodynamic yaw moment in waves
$N_r$	derivative of yaw moment with respect to yaw rate
$N_r^W$	wave effect on the linear derivative of yaw moment with respect to yaw rate
$N_v$	derivative of yaw moment with respect to sway velocity
$N_v^W$	wave effect on the linear derivative of yaw moment with respect to sway velocity
$N_w$	wave-induced yaw moment
$N_\delta$	derivative of yaw moment with respect to rudder Angle
$N_\delta^W$	wave effect on the derivative of yaw moment with respect to rudder angle
$N_\phi$	derivative of yaw moment with respect to roll angle
$\Delta N'$	$\Delta N' = \Delta N / (1/2 \rho L^2 d u^2)$
$p$	roll rate
$r$	yaw rate
$R$	ship resistance
$t$	time
$T$	propeller thrust
$T_D$	time constant for differential control
$T_E$	time constant for steering gear
$T^W$	wave effect on propeller thrust
$u$	surge velocity
$v$	sway velocity
$X_{NL}^M$	nonlinear manoeuvring forces in surge
$X_{NL}^R$	nonlinear heel-induced hydrodynamic surge force in still water
$X_w$	wave-induced surge force
$X_{rud}$	rudder-induced surge force
$\Delta X'$	$\Delta X' = \Delta X / (1/2 \rho L d u^2)$
$Y_{NL}^M$	nonlinear manoeuvring forces in sway
$Y_{NL}^R$	nonlinear heel-induced hydrodynamic sway force in still water
$Y_{NL}^{RW}$	nonlinear heel-induced hydrodynamic sway force in waves
$Y_r$	derivative of sway force with respect to yaw rate
$Y_r^W$	wave effect on the derivative of sway force with respect to yaw rate
$Y_v$	derivative of sway force with respect to sway velocity
$Y_v^W$	wave effect on the derivative of sway force with respect to sway velocity
$Y_w$	wave-induced sway force
$Y_\delta$	derivative of sway force with respect to rudder angle
$Y_\delta^W$	wave effect on the derivative of sway force with respect to rudder angle
$Y_\phi$	derivative of sway force with respect to roll angle
$\Delta Y'$	$\Delta Y' = \Delta Y / (1/2 \rho L d u^2)$
$z_H$	vertical position of centre of sway force due to lateral motions
$\chi$	heading angle from wave direction
$\chi_c$	desired heading angle for auto pilot
$\delta$	rudder angle
$\phi$	roll angle
$\lambda$	wave length
$\theta$	pitch angle
$\rho$	water density
$\xi_G$	longitudinal position of centre of gravity from a wave trough
$\zeta_G$	vertical distance between centre of gravity and still water plane

## REFERENCES

1. Umeda, N., Matsuda, A., Hamamoto, M. and Suzuki, S. 1999. "Stability Assessment for Intact Ships in the Light of Model Experiments" *Journal of Marine Science and Technology*, 4:2: 45-57.
2. Umeda, N. and Renilson, M.R. 2001. "Benchmark Testing of Numerical Prediction on Capsizing of Intact Stability in Following and Quartering Seas" *Proceedings of the 5th International Stability Workshop*, 6.1.1-10.
3. Renilson, M.R. and Manwarring, T. 2000. "An Investigation into Roll/Yaw Coupling and Its Effect on Vessel Motions in Following and Quartering Seas" *Proceedings of the 7th International Conference on Stability and Ocean Vehicles*, 452-459.
4. Nakato, M. and Kohara, S. 1982. "Stability Experiments in the Following Sea with Ship Speed –An Utilization of Circulating Water Channel–" *Proceedings of the 2nd International Conference on Stability and Ocean Vehicles*, 399-410.
5. Umeda, N. and Renilson, M.R. 1992. "Broaching -a dynamic behaviour of a vessel in following seas-" *Wilson PA (ed) Manoeuvring and control of marine craft*, Computational Mechanics Publications, 533-543.
6. Umeda, N. 1999. "Nonlinear dynamics of ship capsizing due to broaching in following and quartering seas" *Journal of Marine Science and Technology*, 4:1: 16-26.
7. Hashimoto, H., Umeda, N. and Matsuda, A. 2004. "Importance of Several Nonlinear Factors on Broaching Prediction" *Journal of Marine Science and Technology*, 9:2: 80-93.
8. Umeda, N., Hashimoto, H. and Matsuda, A. 2002. "Broaching Prediction in the Light of an Enhanced Mathematical Model with Higher Order Terms Taken into Account" *Journal of Marine Science and Technology*, 7:3: 145-155.
9. Grim, O. 1961. "Beitrag zu dem Problem der Sicherheit des Schiffes im Seegang" *Shiff und Hafen*, 6: 490-497 (in German)
10. Umeda, N. and Hashimoto, H. 2002. "Qualitative Aspects of Nonlinear Ship Motions in Following and Quartering Seas with High Forward Velocity" *Journal of Marine Science and Technology*, 6:2 111-121.

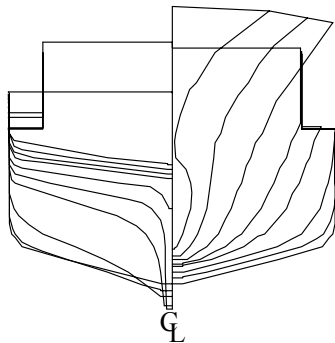


Fig.1 Body plan of the subject ship

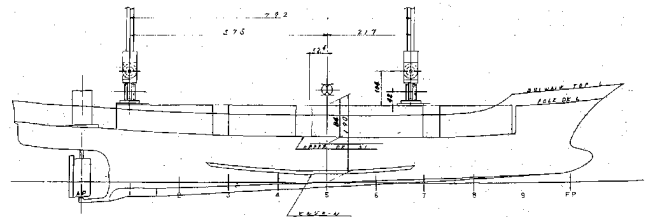


Fig.2 General arrangement of the purpose-built ship model

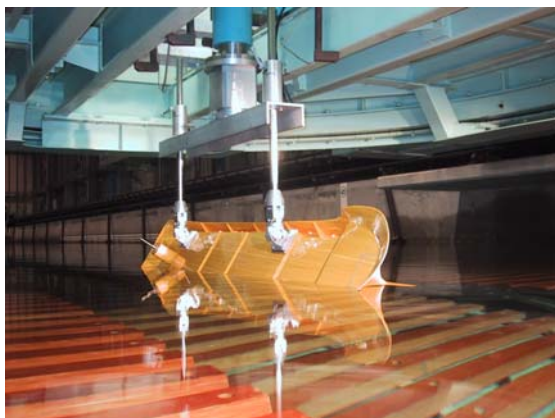


Fig.3 Setup of the captive model experiment

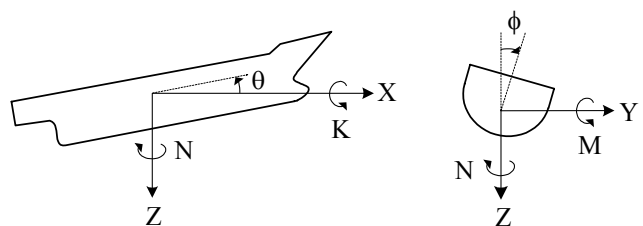


Fig.4 Definition of directions of the measured forces and moments



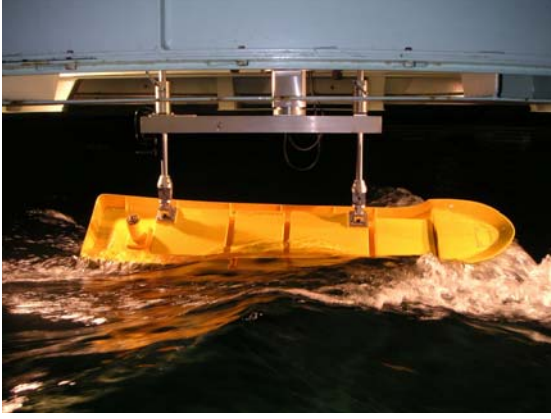


Fig.5 A photograph of captive test in waves

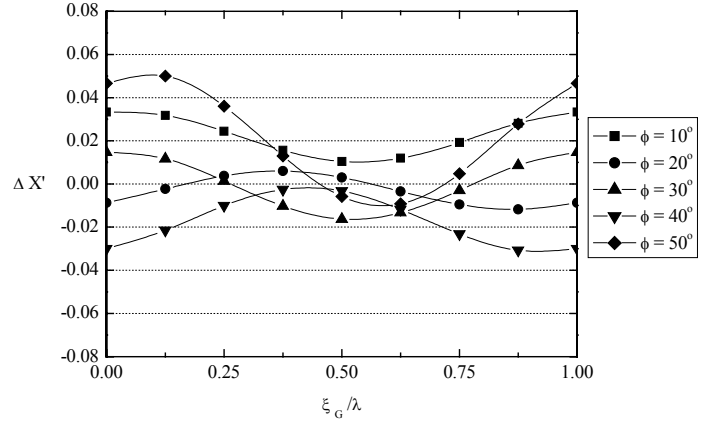


Fig.6 Experimental result of non-dimensional heel-induced surge force with  $H/\lambda=1/10$ ,  $\lambda/L=1.637$ ,  $\chi=0^\circ$  and  $Fn=0.4$

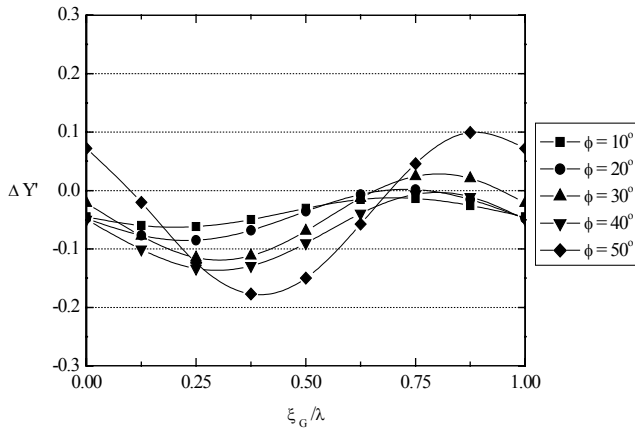


Fig.7 Experimental result of non-dimensional heel-induced sway force with  $H/\lambda=1/10$ ,  $\lambda/L=1.637$ ,  $\chi=0^\circ$  and  $Fn=0.4$

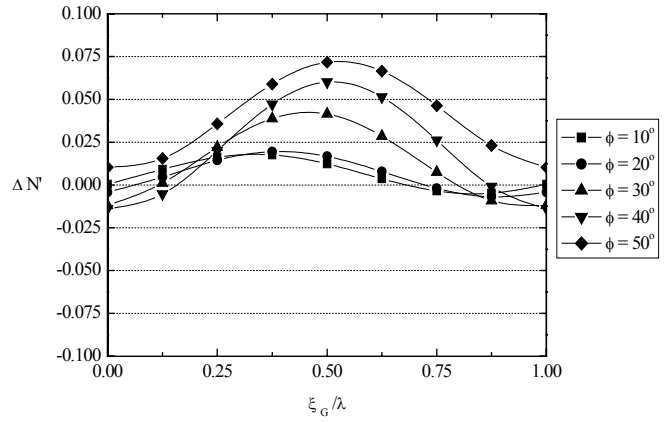


Fig.8 Experimental result of non-dimensional heel-induced yaw moment with  $H/\lambda=1/10$ ,  $\lambda/L=1.637$ ,  $\chi=0^\circ$  and  $Fn=0.4$

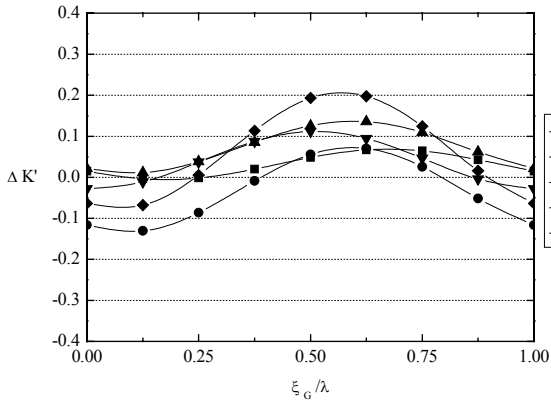


Fig.9 Experimental result of non-dimensional heel-induced roll moment with  $H/\lambda=1/10$ ,  $\lambda/L=1.637$ ,  $\chi=0^\circ$  and  $Fn=0.4$

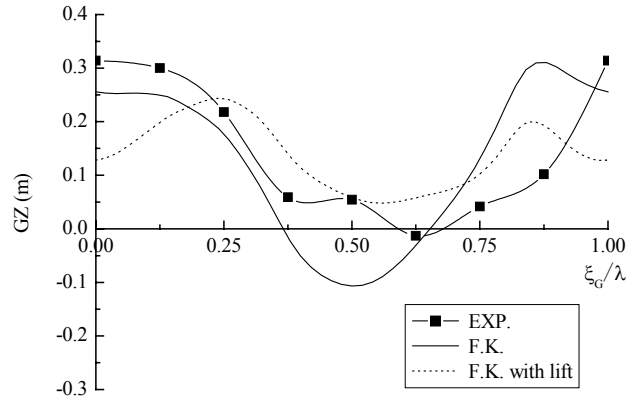


Fig.10 Comparison of righting arm in waves between the experiment, the Froude-Krylov calculation and the sum of Froude-Krylov calculation and experimental formula of lift effect with  $H/\lambda=1/10$ ,  $\lambda/L=1.637$ ,  $\chi=0^\circ$ ,  $Fn=0.4$  and  $\phi=20^\circ$  degrees

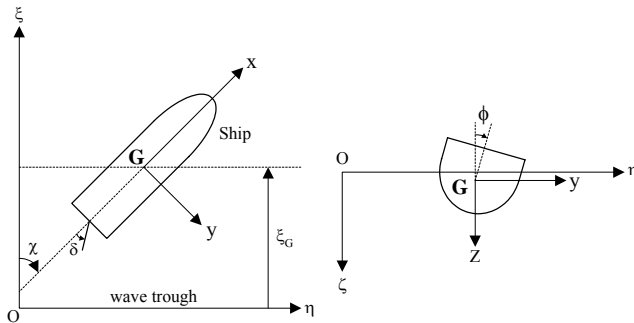


Fig.11 Co-ordinate systems

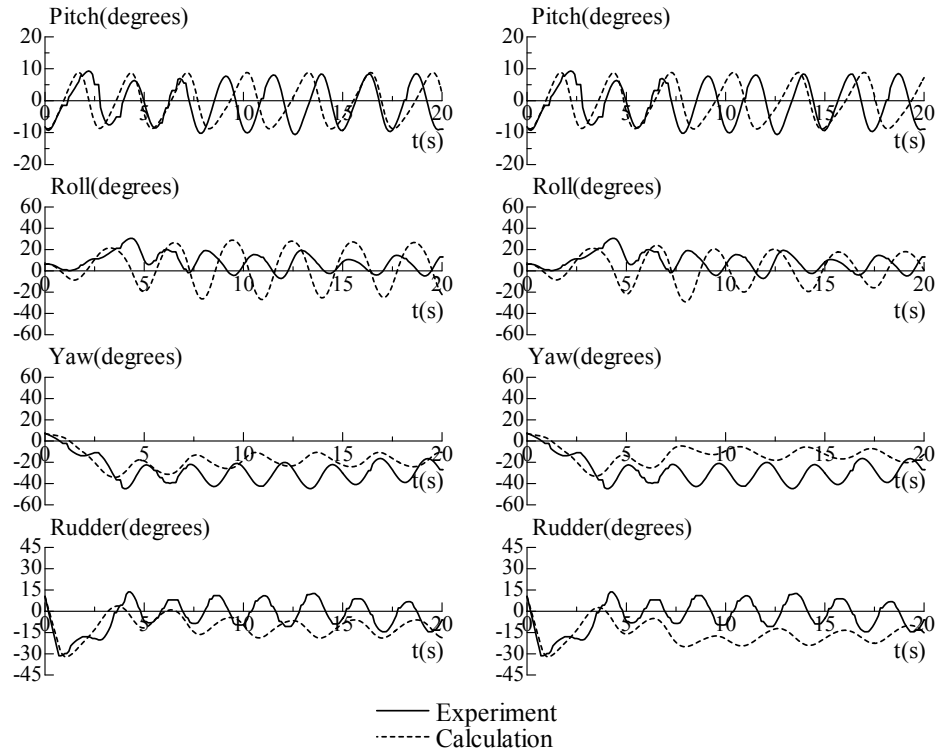


Fig.12 Comparison of numerical results with  $H/\lambda=1/10$ ,  $\lambda/L=1.637$ ,  $F_n=0.3$ ,  $\chi_c=-30$  degrees. (left: without heel-induced hydrodynamic sway force and yaw moment in waves, right: with them)

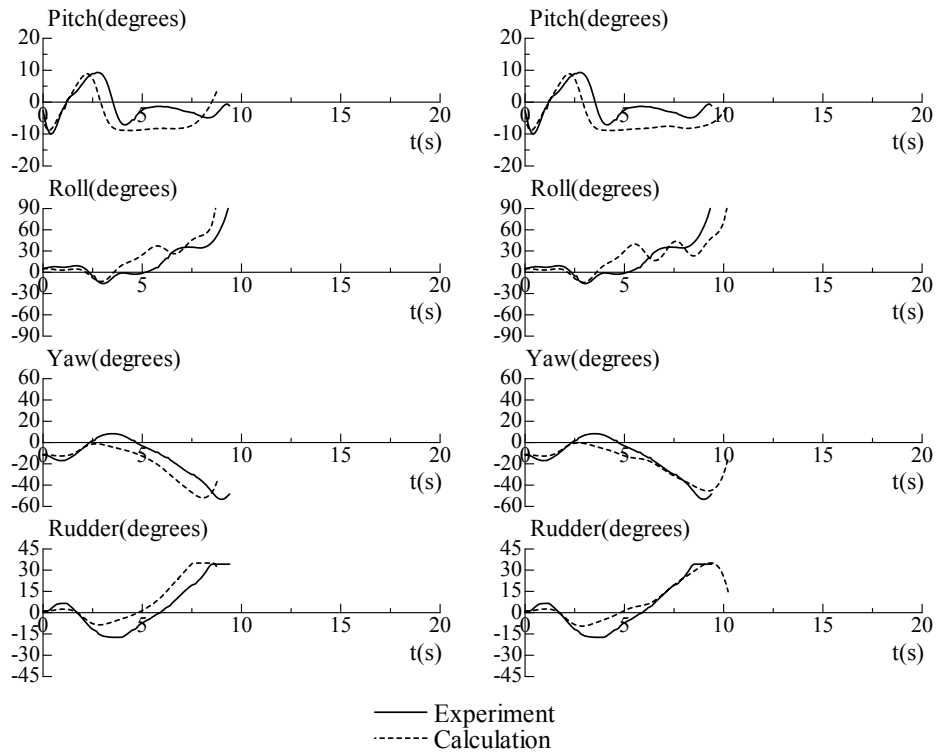


Fig.13 Comparison of numerical results with  $H/\lambda=1/10$ ,  $\lambda/L=1.637$ ,  $F_n=0.43$ ,  $\chi_c=-10$  degrees. (left: without heel-induced hydrodynamic sway force and yaw moment in waves, right: with them)

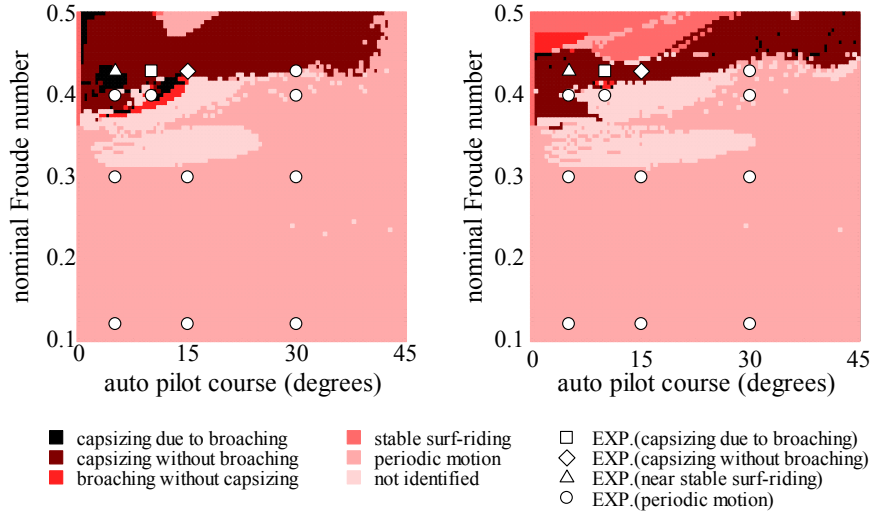


Fig.14 Comparison of boundaries of ship motion modes with  $H/\lambda=1/10$ ,  $\lambda/L=1.637$  and the initial periodic state for  $F_n=0.1$  and  $\chi_c=0$  degrees. (left: without heel-induced hydrodynamic sway force and yaw moment in waves, right: with them)

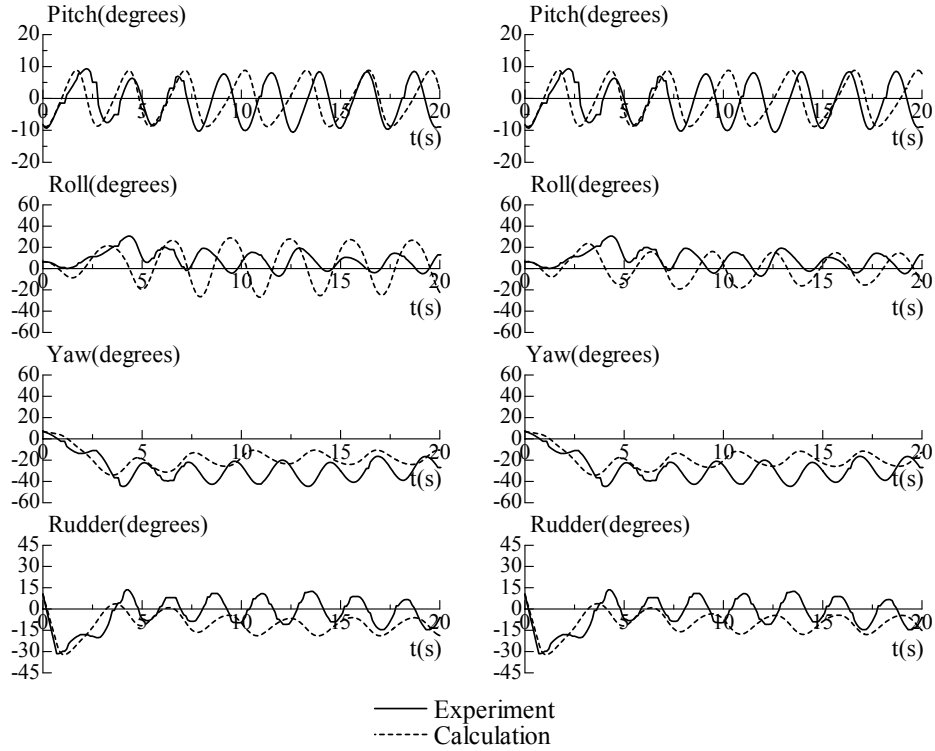


Fig.15 Comparison of numerical results with  $H/\lambda=1/10$ ,  $\lambda/L=1.637$ ,  $F_n=0.3$ ,  $\chi_c=-30$  degrees. (left: with experimentally obtained GZ variation, right: with calculated GZ variation by Froude-Krylov assumption and experimental formula)

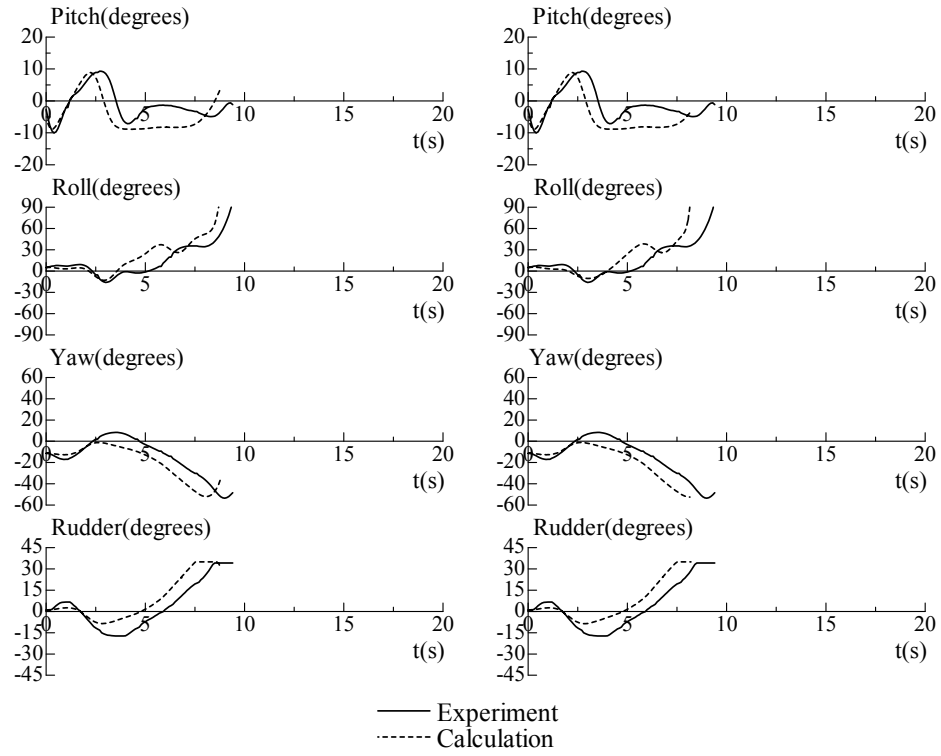


Fig.16 Comparison of numerical results with  $H/\lambda=1/10$ ,  $\lambda/L=1.637$ ,  $F_n=0.43$ ,  $\chi_c=-10$  degrees. (left: with experimentally obtained GZ variation, right: with calculated GZ variation by Froude-Krylov assumption and experimental formula)

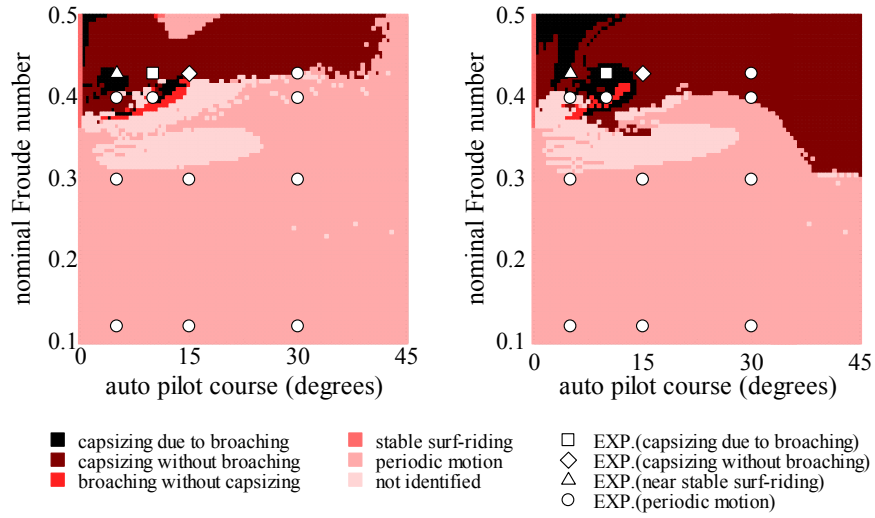


Fig.17 Comparison of boundaries of ship motion modes with  $H/\lambda=1/10$ ,  $\lambda/L=1.637$  and the initial periodic state for  $F_n=0.1$  and  $\chi_c=0$  degrees. (left: with experimentally obtained GZ variation, right: with calculated GZ variation by Froude-Krylov assumption and experimental formula)